Investigation of the Impact of Polarization and Auger Recombination on the Wurtzite and Zincblende GaN-Based Green LEDs

Yi-Chia Tsai[1]

Department of Electrical and Computer Engineering, University of Illinois at Urbana-Champaign, Illinois, 61801, USA
Micro and Nanotechnology Laboratory, University of Illinois at Urbana-Champaign, Illinois, 61801, USA

ABSTRACT

It is challenging to reach high efficiency for wurtzite GaN-based green LEDs. Four factors are surmised to account for the low efficiency: strong polarization field, Auger recombination rate, electron leakage, and thermal effect. These factors inherited from the electronegativity of III-nitride bonds, the small excitation energy in the conduction bands, the limited capture rate of quantum wells, and the increasing escaping rate respectively. To tackle these issues together, the zincblende GaN-based nitrides featuring polarization-free nature and large excitation energy in the conduction bands are promising for the next-generation high-efficiency green LEDs. In this project, the impact of polarization, Auger recombination rate, electron leakage, and thermal effect on the efficiency of wurtzite GaN-based green LEDs are investigated numerically. Next, the materials are replaced by zincblende GaN-based nitrides for further optimizations. The active layers are optimized by benchmarking the number and width of quantum wells. Ultimately, the highest wall-plug efficiencies of wurtzite GaN green LEDs operated under 100A/m (1A/cm) carrier injection is 13.4% using single quantum well with 3 nm thickness; while, the highest wall-plug efficiencies of wurtzite GaN green LEDs operated under 5V is 7.4% using five quantum wells with 3 nm thickness. However, the highest wall-plug efficiencies of zincblende GaN green LEDs operated under 100A/m and 5V are 48.3% and 21.6% using five quantum wells with 11 nm thickness, respectively. Zincblende GaN green LEDs do improve the wall-plug efficiencies by more than a factor of 3. Proven by the simulations, zincblende GaN have shown its material and device advantages over wurtzite GaN, which motivate their applications in LEDs and laser diodes.

I. INTRODUCTION

The lighting technology has undergone a momentous revolution ever since the first light-emitting diode (LED) was invented in 1962[1]. However, not until the invention of high-brightness blue LED in 1994[2], the white LED took place fluorescent light bulb with a higher luminous efficacy. The incumbent technique of white LED is to pump yellow-emitting phosphor with blue LED, which is fabricated by wurtzite GaN[3]. Although wurtzite GaN with a high breakdown voltage, superior electron mobility, and excellent electron saturation velocity are promising for high-power applications, the power dissipation and heat transfer generated at the junction under high-power operation shortens the longevity and decreases the efficiency of GaN devices, especially for LED because the power density of the LED is ten times higher than conventional Si chip. In addition to the power dissipation, wurtzite GaN and its alloys have strong spontaneous and piezoelectric polarization due to the lack of inversion symmetry[4]. As shown in Fig. 1, because of the high-level

[1] Innovative COmpound semiconductoR LABoratory (ICORLAB); Email: yichiat2@illinois.edu;
Webpage: icorlab.ece.illinois.edu; Phone: +1 (217) 300-0978; Fax: +1 (217) 244-6375

indium content and strong polarization, GaN-based green LED is 4 times less efficient than red and blue LEDs, which is described as "green gap"[5]. The low efficiency of the green emission impedes the development of natural white-light spectra with a high-power efficiency.

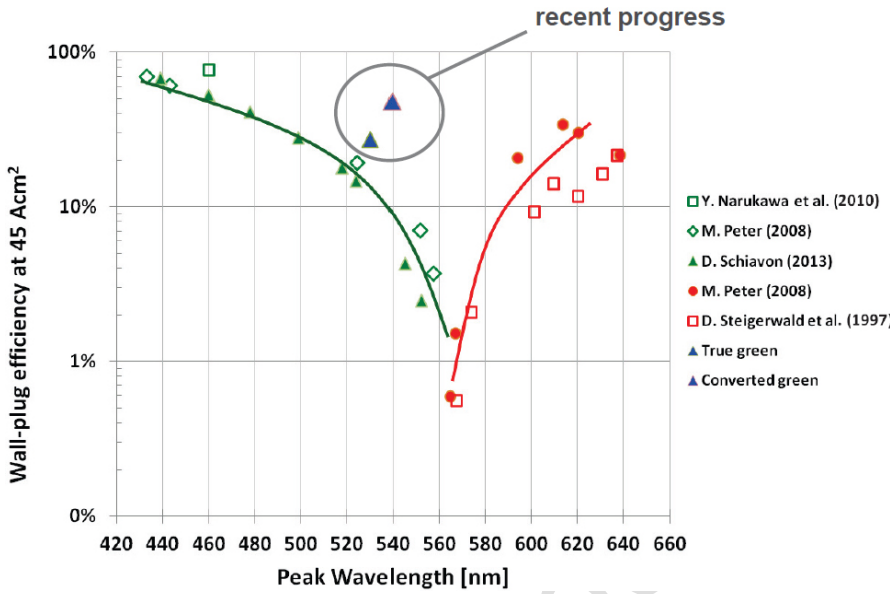

Fig. 1 LED wall-plug efficiency as a function of wavelength. The efficiency gap ranges from 520 to 580 nm, which overlaps the green wavelength between 495 and 570 nm[6].

Raising the driving current of LEDs is a common approach to increase the brightness of LEDs. However, the efficiency drops when the driving current goes higher than tens of mA. The phenomenon called efficiency droop. Although efficiency droop is common in LEDs under high-power operation, it further deteriorates the efficiency of green LEDs. Although several mechanisms, such as electron leakage, thermal transport, and non-radiative recombination processes, may account for the efficiency droop, it is prohibitively challenging to distinguish different kind of non-radiative recombination mechanisms in experiment. Nonetheless, Auger recombination process is widely believed to be the major culprit that limits the controllability of the driving current on the luminous flux of LED[7]. Theoretical studies are, therefore, essential to identify the contributions from each mechanism to the efficiency droop so that the efficiency of LEDs can be optimized.

To address the green gap issue and efficiency droop simultaneously, the zincblende GaN is adopted because the zincblende GaN, in theory, has a lower Auger coefficient which leads to a lower Auger losses[8]. Given zincblende symmetry, zincblende GaN has a polarization-free nature. Accompanied with a smaller bandgap than the wurtzite counterparts, zincblende GaN is a promising solution to close green gap and minimize the efficiency droop in LEDs. In this project, I first recover the green gap issue in the simulate and analyze the impact of polarization, different recombination mechanisms, electron leakage, and thermal effect that contributes to the green gap issue. Second, the active layer is optimized for wurtzite GaN green LEDs by varying the number and thickness of quantum wells. Eventually, zincblende GaN and InGaN is employed to further optimize the efficiency of green LEDs.

II. METHODS

The quantum-corrected drift-diffusion model is exploited to simulate the I-V characteristics and carrier transport properties of LEDs, which consists of three fundamental equations. First of all, the Poisson equation will be applied to calculate the electrostatic potential profile (ϕ) of LEDs expressed by:

$$\nabla \cdot \left(\varepsilon_0 \nabla \phi + \vec{P} \right) = -q \left(p - n + N_D - N_A + n_p \right),$$

where ε_0, q, p, n, N_D, and N_A are static dielectric constant, elementary charge, hole density, electron density, donor concentration, and acceptor concentration; while, $\vec{P}$ is the polarization contributed from spontaneous and piezoelectric polarization and n_p is the polarization-induced sheet charge. To consider the quantization of quantum wells, Schrödinger equation is used to correct ϕ, p, and n in the quantum wells so-called self-consistent Schrödinger–Poisson simulation. The confined energy-states are expressed as:

$$-\frac{\hbar^2}{2m^*} \nabla^2 \psi_i + e\phi\psi_i = E_i \psi_i .$$

The carrier density, for example n, in the quantum well is given by:

$$n = 2 \sum_i f \left(E_i - E_F \right) \left| \psi_i \right|^2 ,$$

where f, E_F, E_i, and ψ_i are Fermi-Dirac distribution, Fermi level, the i^{th} confined energy-state, and the corresponding wavefunction, respectively. The second equations are used to formulate carrier dynamics by drift and diffusion contributions. The electron ($\vec{J}_n$) and hole ($\vec{J}_p$) current densities can be formulated by

$$\vec{J}_n = q\mu_n n\vec{E} + qkT\mu_n \nabla n,$$
$$\vec{J}_p = q\mu_p p\vec{E} - qkT\mu_p \nabla p,$$

where μ_n, μ_p, $\vec{E}$, k, and T are electron mobility, hole mobility, electric field, Boltzmann constant, and temperature, respectively. Notably, the electron and hole diffusion coefficients are expressed by electron and hole mobilities using Einstein relation, respectively. These two equations are enough to give a good expression in the equilibrium condition of a PN junction, where the carrier generation and recombination are counterbalanced. However, there are three dominant carrier recombination processes–Shockley–Read–Hall recombination (R_{SRH}), radiative recombination (R_{Rad}), and Auger recombination (R_{Auger}) during LED operation. Therefore, the electron and hole continuity equations under steady-state condition are solved to include the impact of carrier recombination on carrier dynamics, where the equations are formulated by

$$\frac{1}{q}\nabla \cdot \vec{J}_n = R^n{}_{SRH} + R_{Rad} + R_{Auger},$$
$$-\frac{1}{q}\nabla \cdot \vec{J}_p = R^p{}_{SRH} + R_{Rad} + R_{Auger}.$$

R_{SRH} is the Shockley–Read–Hall recombination rate. For example, the Shockley–Read–Hall recombination rate for electron can be expressed by

$$R^n{}_{SRH} = \frac{n(1-f_t) - n_1 f_t}{\tau_n},$$

where n_1, f_t, and τ_n are the electron concentration when the electron quasi-Fermi level coincides with the trap state, the Fermi-Dirac distribution on trap, and SRH carrier lifetime for electron, respectively. The Shockley–Read–Hall recombination rate for hole has the similar expression. It worth mentioning that the SRH carrier lifetimes for electron and hole are set as 100 ns in the simulations based on experimental extraction[9]. R_{Rad} is the radiative recombination rate, which can be expressed as

$$R_{Rad} = B(np - n_i^2),$$

where B is the radiative coefficient that is set as $2 \cdot 10^{-11}$ cm^3s^{-1} for both wurtzite and zincblende GaN. Finally, the Auger recombination rate (R_{Auger}) is formulated by

$$R_{Auger} = (C_n n + C_p p)(np - n_i^2),$$

where C_n and C_p are the Auger coefficients for electron and hole, respectively. According to widely accepted values[10], $2.96 \cdot 10^{-30}$ cm^6s^{-1} is chosen for both C_n and C_p. Notably, although the band structure of zincblende GaN indicates that it has a lower Auger coefficient than wurtzite GaN, there is still no experimental and theoretical value for reference. Therefore, the Auger coefficients of zincblende GaN and InGaN are assumed to be identical to the wurtzite GaN.

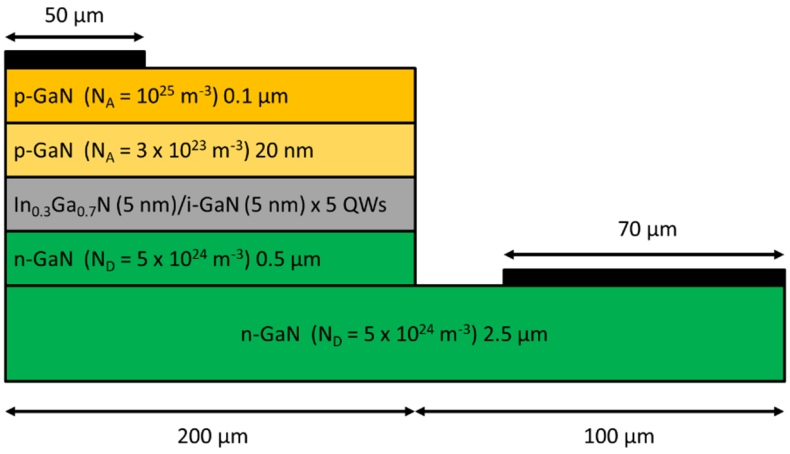

Fig. 2 Illustration of the device structure of green LED with 5 QWs.

III. RESULTS AND DISCUSSION

In this project, the active layers are constructed by multiple intrinsic $In_{0.3}Ga_{0.7}N$ quantum wells and sandwiched by p- and n-junctions. The In mole fraction of 0.3 is calculated using Vegard's law so that the bandgap emits a green wavelength of 550 nm without the consideration of quantization effect. Fig. 2 illustrates the device structure of green LEDs with 5 QWs. The doping concentration on p-layer and n-layer are 10^{25} m^{-3} and 5 x 10^{24} m^{-3}, respectively. Notably, because the hole mobility of GaN is 5 times smaller than that of the electron mobility, the thickness of p-layer is designed to be 120 nm only to minimize the hole traveling time before being captured by quantum wells. Fig. 3 exemplifies the band diagram and carrier injection of wurtzite (hexagonal) GaN and zincblende (cubic) GaN green LEDs.

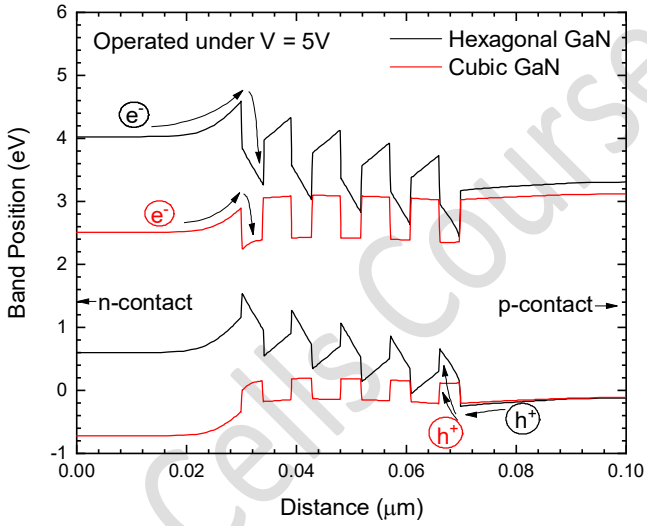

Fig. 3 Exemplification of the band diagram and carrier injection of wurtzite (hexagonal) GaN and zincblende (cubic) GaN green LEDs.

- **GREEN GAP ANALYSIS**

To begin with, the factors that contributes to the green gap are investigated and identified. Fig. 4 demonstrated the spontaneous emission rate and peak wavelength of LEDs with respect to the In mole fraction of active layer operated under 5V bias. The active layer is constructed by single QW with a thickness of 2.5 nm. The peak wavelength is red shifted with the increasing In mole fraction because the bandgap of active layer becomes smaller. However, the spontaneous emission rate is reduced with respect to the increasing In mole fraction, which indicates the reduction of optical power. Fig. 5 shows the optical power emitted from the active layer with respect to different In mole fraction under different rate of carrier injections. Although the optical power increases with the increasing carrier injection rates, the figure does shows that the optical power drops with the increasing In mole fraction, except for the 0.1 In mole fraction. To understand what causes the reduction of optical power and spontaneous emission rate, the impacts of non-radiative and

radiative recombination rates, electron leakage, polarization, and thermal effect on optical power and efficiency are examined individually.

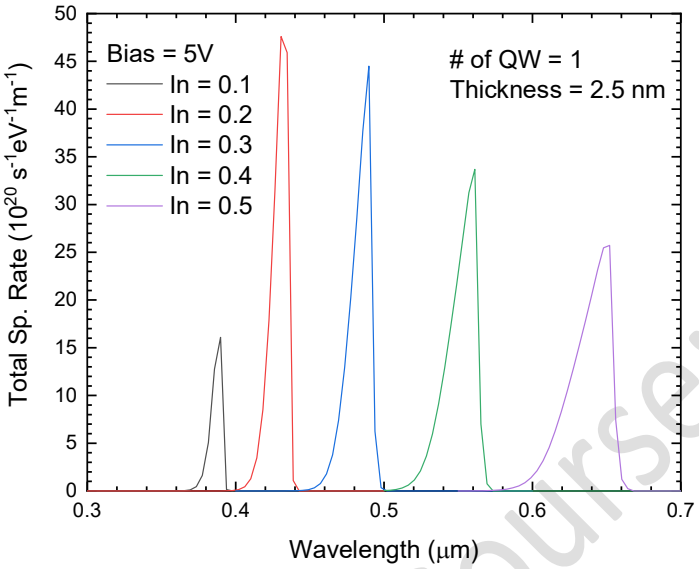

Fig. 4 Spontaneous emission rate with respect to the In mole fraction of active layer operated under 5V bias. The active layer is constructed by single QW with a thickness of 2.5 nm.

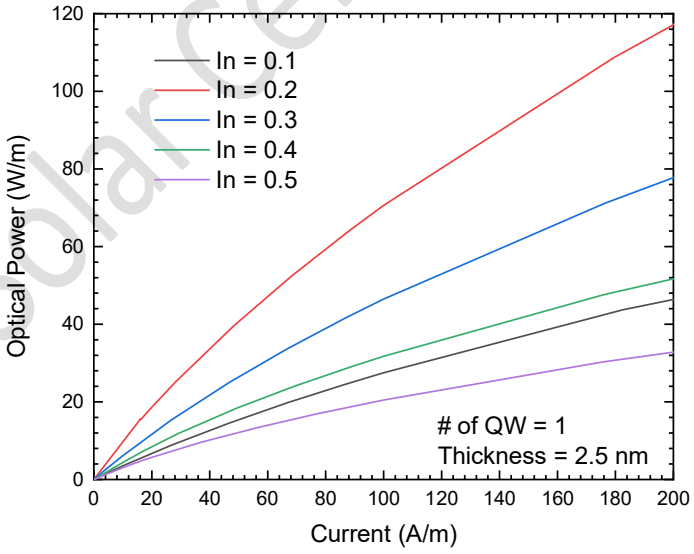

Fig. 5 Optical power with respect to the In mole fraction of active layer operated under different carrier injections. The active layer is constructed by single QW with a thickness of 2.5 nm.

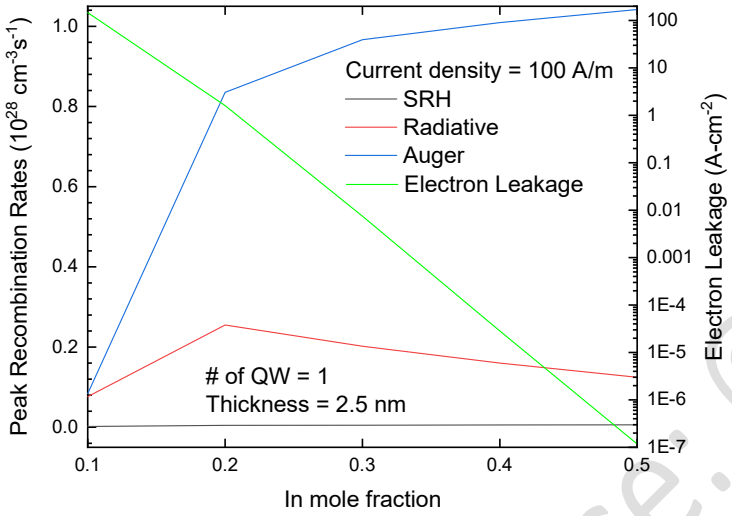

Fig. 6 Peak SRH, radiative, Auger recombination rates, and electron leakage as a function of In mole fractions operated under 100A/m carrier injection.

Fig. 6 extracts the peak SRH, radiative, Auger recombination rates, and electron leakage as a function of In mole fractions operated under 100A/m carrier injection. It shows that the high electron leakage is the major culprit for 0.1 In mole fraction to have a low optical power and spontaneous emission. The high electron leakage can be attributed to the low capture rate caused by the narrow and shallow QW. By increasing the In mole fraction, the leakage current drops exponentially because of the deeper QW and a higher capture rate. However, as the QW goes deeper, the Auger recombination rate increases drastically because the confined electron concentration increases exponentially. Additionally, the spontaneous and piezoelectric polarization fields slant QW more significantly in a deep QW than a shallow QW, which results in a severer electron-hole separation known as quantum-confined Stark effect. As the consequence, the radiative recombination rate drops with respect to the increasing In mole fraction even if the electron concentration is high. From the results, the SRH recombination almost remains constant, which indicates that green gap is not caused by SRH recombination. To understand how the polarization field affects the radiative recombination rate, Fig. 7 exhibits the internal quantum efficiency (IQE) as function of current density for different In mole fraction with and without the polarization field. It shows that the IQE with polarization field is high for low carrier injection because the narrow QW accompanied with polarization field forms a triangular quantum well, which helps the localization of electron and hole wavefunction and improves the electron-hole overlap integral. However, it happens only for narrow QWs with low carrier injection, if the current increases due to a stronger external bias, the external electric field is going to slant the QW further and strengthens the quantum-confined Stark effect. As the consequence, the IQE with polarization drops below the ones without polarization after the carrier density is approximately greater than 100 A/m. Under the assumption of the same bandgap, band offset, and Auger coefficients the impact of polarization on IQE is between 3% and 5% depending on the carrier injection rate.

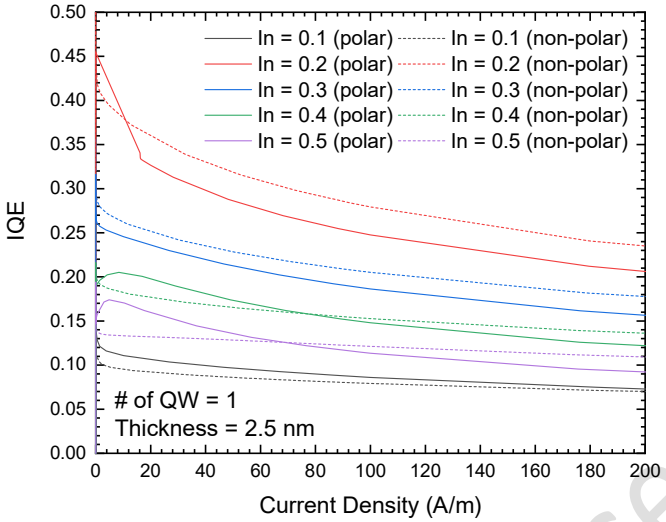

Fig. 7 Internal quantum efficiency (IQE) as function of current density for different In mole fraction with and without the polarization field.

It is clear that Auger recombination plays a pivot role in the deterioration of IQE and optical power, the phenomenon is known as "efficiency droop". Fig. 8 shows the sensitivity of efficiency droop on the assigned Auger coefficient ($2.96 \cdot 10^{-30}$ cm^6s^{-1}) by varying its order from $2.96 \cdot 10^{-33}$ to $2.96 \cdot 10^{-28}$ cm^6s^{-1}. The result shows that IQE can get an improvement by a factor of 2 if the Auger coefficient is reduced by 1 order. Additionally, the droop-free performance can be achieved if the Auger coefficient is reduced by more than 2 orders. On the contrary, if the Auger coefficients in increased by more than an order, the IQE drops below 5%, indicating that an order difference in the Auger coefficient may cause significant impact on the efficiency of green LEDs. It is technologically important to find a material that has low Auger coefficient for first droop-free and high-efficiency green LEDs. Finally, it is important to understand how the thermal energy affects the IQE because the thermal accumulation in the active layer is the major issue that degrades the longevity and efficiency of LEDs. Fig. 9(a) shows the IQE as a function of current density under different temperature conditions ranging from 250K to 500K. It shows that the IQE drops monotonically as the temperature increases. For example, the IQE of the device operated under 200 A/m and 250K is 0.176, which is 0.07 greater than the device operated under the same carrier injection rate with a temperature of 500K. On average, 100K increase in temperature leads to 2.8% reduction in IQE, which is minimal in comparison with the impact of Auger coefficient and polarization on IQE. To understand how the increasing temperature decreases the IQE, Fig. 9(b) summarizes the peak recombination rates in the QW (left-y axis) and electron leakage (right-y axis) as a function of temperature under 100A/m carrier injection rate. It shows that the increasing temperature enhances the electron leakage because electrons are not likely to be captured by QW. Once they were captured, the electrons still have a higher probability to escape the QW by absorbing thermal energy. As the consequence, the electron concentration in the QW drops, which leads to the reduction of radiative recombination rate. However, the Auger recombination rate doesn't drop with the decreasing electron concentration because of the increasing hole

concentration. The hole mobility is 5 times slower than that of electron mobility, therefore, the increase of temperature improves the hole mobility and reduces the chance of SRH recombination before capturing by the QW. As the result, the hole concentration in the QW increases and enhances the Auger recombination for hole because it has a quadratic dependence on the hole concentration.

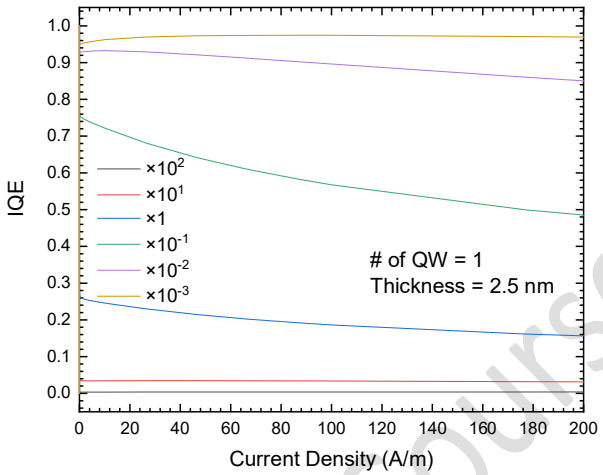

Fig. 8 The sensitivity of efficiency droop on the assigned Auger coefficient ($2.96 \cdot 10^{-30}$ cm^6s^{-1}) by varying its order from $2.96 \cdot 10^{-33}$ ($\times 10^{-3}$) to $2.96 \cdot 10^{-28}$ ($\times 10^{2}$) cm^6s^{-1}.

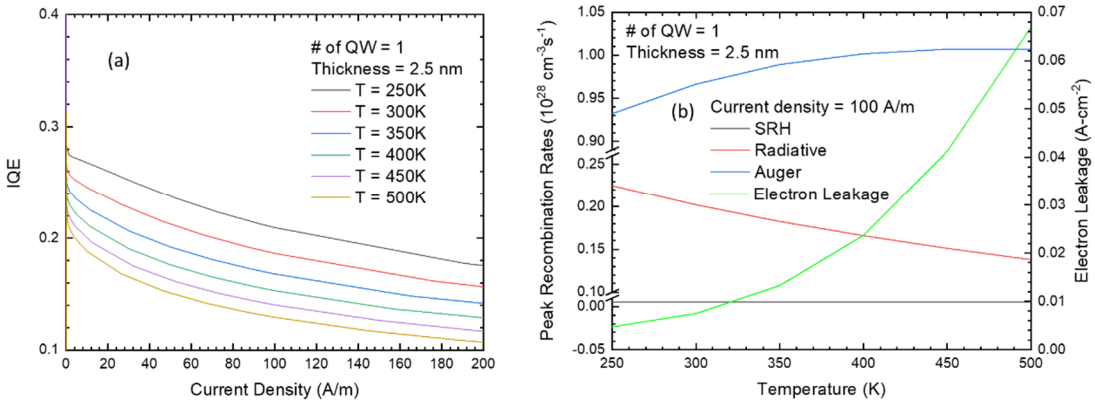

Fig. 9 (a) IQE as a function of current density under different temperature conditions ranging from 250K to 500K. (b) Peak recombination rates in the QW (left-y axis) and electron leakage (right-y axis) as a function of temperature under 100A/m carrier injection.

So far, where the green gap issue originates from has been identified. Auger recombination, electron leakage, polarization, and thermal effect have a nonnegligible impact on the low efficiency of green emission. The improvement of Auger coefficient and polarization necessitates a fundamental material engineering; while, radiative recombination rate and electron leakage can

be improved with a better QW design. Thermal effect can be improved using a better substrate with a high thermal conductivity and high thermal boundary conductance. I am going to improve the green gap by engineering the device structure and its material in the following sections.

- **OPTIMIZATION OF WURTZITE GAN-BASED GREEN LEDS**

In this section, the wurtzite GaN-based green LEDs are optimized by introducing more QWs with different QW thicknesses. Specifically, the numbers of QW from 1 to 5 are focused; while, the QW thickness ranges from 1 nm to 5 nm. The introduction of multiple QWs and wide QW thickness is able to increase the capture rate and the electron concentration in the QWs, which can effectively reduce the electron leakage. However, the confined energy-states also depend on the QW structures. Fig. 10(a) and (b) extracts the peak emission wavelength and the corresponding spontaneous emission rate.

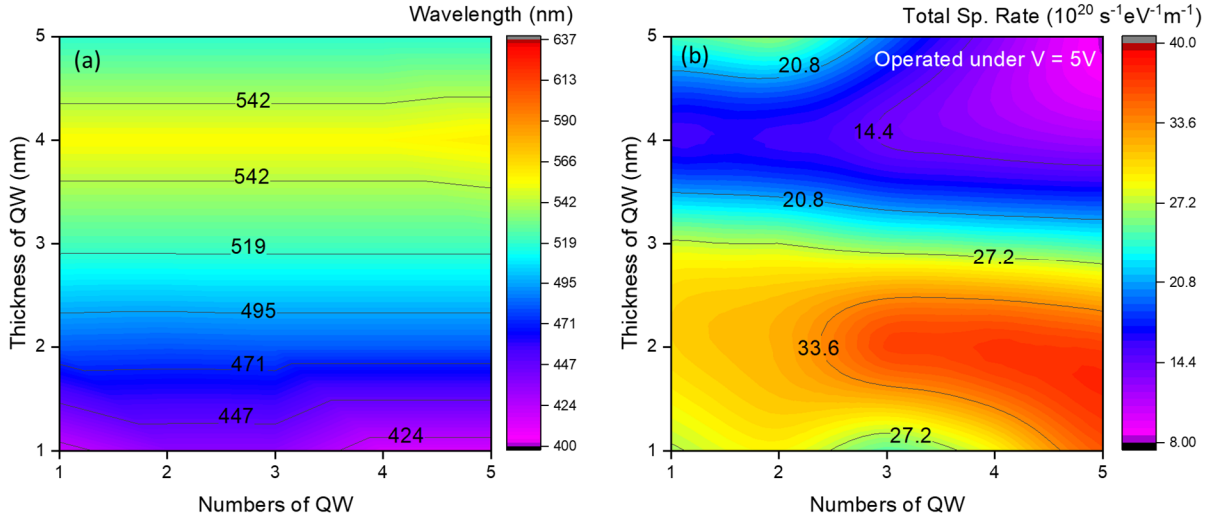

Fig. 10 (a) Peak emission wavelength and (b) the corresponding spontaneous emission rate of wurtzite GaN-based LEDs.

Although the In mole fraction of 0.3 is designed to target 550 nm wavelength emission in the active layer, the formation of quantized energy-states increases the effective bandgap, which leads to the reduction of the wavelength. From Fig. 10(a), the QW thickness larger than 3 nm guarantees the green emission wavelength. On the contrary, if the QW thickness is narrow (with the thickness thinner than 2 nm), a blue emitter can be achieved. However, the spontaneous emission rate reduces with the increasing numbers and thickness of QW, which suggests that there is an optimal design and the highest efficiency that can be achieved. To explain how the spontaneous emission rate is degraded, Fig. 11(a)–(d) demonstrates the integrated SRH, radiative, and Auger recombination rates and electron leakage of wurtzite GaN-based LEDs as a function of the numbers and thickness of QW under 100A/m carrier injection rate. Different from the analysis of a single QW, the peak recombination rate is not enough to benchmark multiple QWs. The peak recombination rate decreases with the increasing number of QW because the confined electrons are shared by multiple QWs, which leads to the reduction of electron concentration in the

individual QW. On the contrary, the integrated recombination rate considers the total recombination rate contributed from individual QW, which can be expressed by

$$R_{int} = \int R(y)dy,$$

where $R(y)$ is the position-dependent recombination rate; while, y is the direction perpendicular to the active layer.

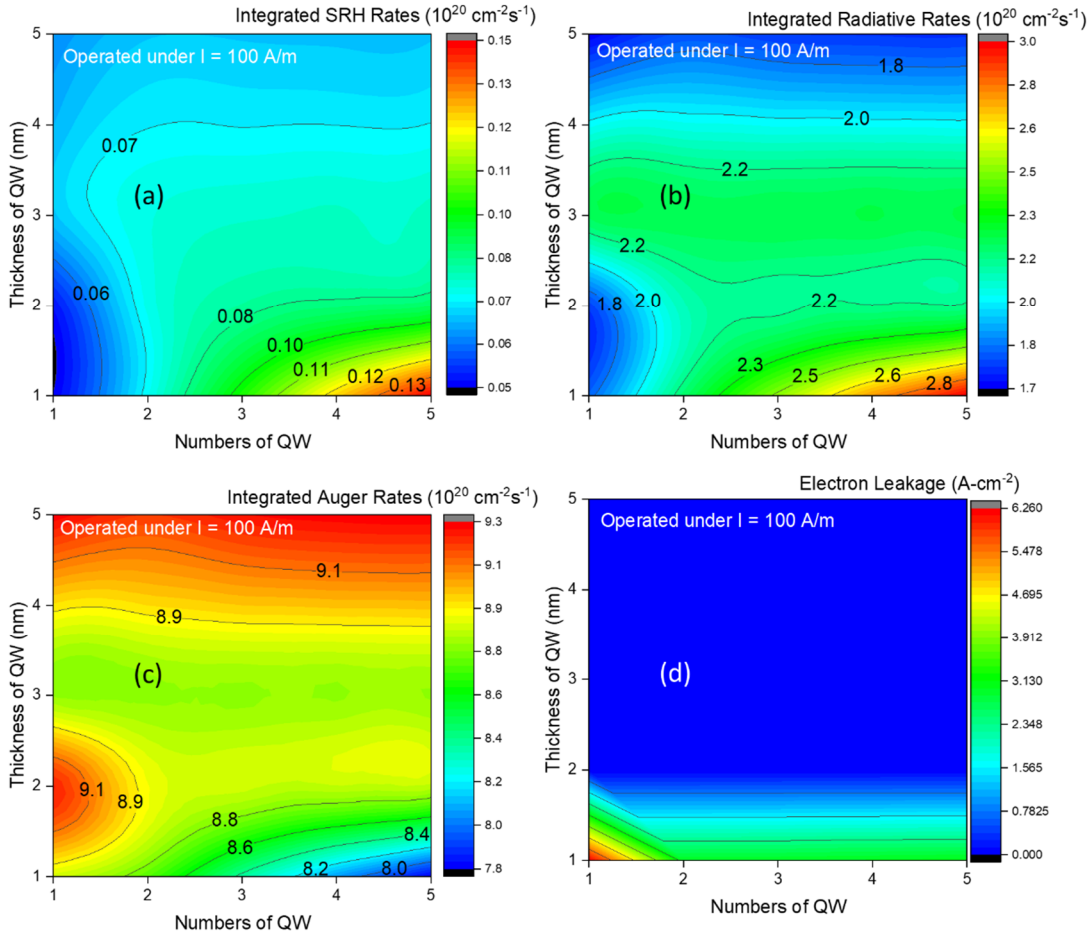

Fig. 11 (a) Integrated SRH, (b) radiative, and (c) Auger recombination rates and (d) electron leakage of wurtzite GaN-based LEDs as a function of the numbers and thickness of QW under 100A/m carrier injection rate.

The figures show that both the SRH and radiative recombination rates decrease with the increasing QW thickness because the quantum-confined Stark effect causes the spatial separation of electron and hole, the quantum-confined Stark effect is more significant in a deep and wide QW, which explain the scenario. As the result, the radiative recombination rate drops when the thickness of QW is greater than 3.5 nm. On the contrary, the maximum radiative recombination rate occurs when the number and thickness of QW are 5 and 1 nm, respectively, because the narrow QW is free of quantum-confined Stark effect; while, the low capture rate of the narrow QW can be

compensated by introducing multiple QWs. The Auger recombination rate, however, increases with the increasing thickness of QW because more electrons can be captured in thick QWs. Despite of the fact that the quantum-confined Stark effect may degrade the electron-hole recombination process and cause the reduction of Auger recombination rate as well, however, the Auger recombination rate is cubically dependent on the electron and hole concentrations, which implies that the Auger recombination rate is dominated by electron and hole concentrations rather than the spatial separation of electrons and holes. The increase of Auger recombination rate with respect to the thickness of QW also indicates that the optimal thickness of QW is bounded and should be smaller than 4 nm. The final factor–electron leakage–shows that the leakage current can be significantly reduced if the thickness of QW is thicker than 2 nm. According to Fig. 11(a)–(d), the numbers of QW have a limited impact on the recombination processes once the thickness is thicker than 3 nm because most of carriers can be captured by a 3-nm thick QW under 100 A/m carrier injection. On the contrary, more QWs are required to strengthen the capture rate of narrow QWs. Overall, SRH and radiative recombination rates are vulnerable to the quantum-confined Stark effect; while, Auger recombination is dominated by carrier concentrations.

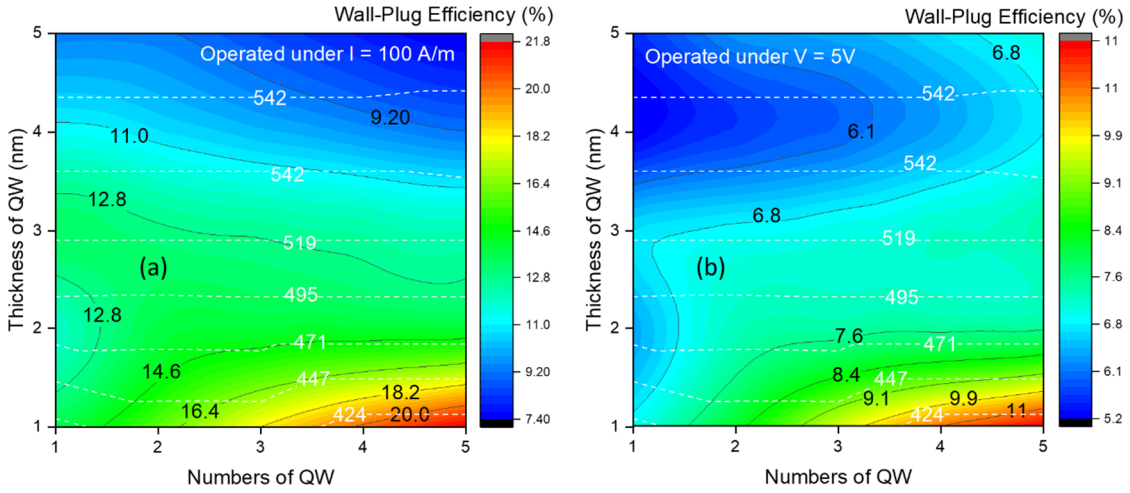

Fig. 12 Wall-plug efficiency of wurtzite GaN-based LEDs as a function of the numbers and thickness of QW under (a) a constant carrier injection of 100 A/m and (b) a constant bias of 5V, respectively. White dash lines indicate the peak emission wavelength.

To summarize the impact of difference recombination processes, electron leakage, QW/barrier resistance on I-V characteristics, optical power, and IQE, the wall-plug efficiency is calculated. Several steps are required to obtain the wall-plug efficiency. First of all, the device can be operated under a constant carrier injection or a constant bias. Next, the input power can be calculated from the I-V characteristics for a given constant carrier injection or a constant bias. Finally, the wall-plug efficiency is calculated by the ratio between the optical power and the input power. Fig. 12 (a) and (b) demonstrates the wall-plug efficiency of wurtzite GaN-based LEDs as a function of the numbers and thickness of QW under a constant carrier injection of 100 A/m and a constant bias of 5V, respectively. Notably, all of the devices are operated between 2V and 4V under a constant carrier injection of 100 A/m. Therefore, a constant bias of 5V represents high carrier injection

because the carrier injection is greater than 100 A/m by a factor of 3. White dash lines indicate the peak emission wavelength. For both operation modes, the wall-plug efficiencies reduce significantly when the thickness of QW is thicker than 3.5 nm because of the reduction of radiative recombination–caused by polarization– and the increase of Auger recombination–caused by high carrier concentration, as explained in Fig. 11. Thus, the optimal thickness of QW for green emitter, where the wavelength is between 500 and 550 nm, is 3 – 3.5 nm. However, the optimal numbers of QW for Fig. 12(a) and (b) are different. In the constant carrier injection of 100 A/m, most of the carriers can be captured by a 3-nm thick QW under 100 A/m carrier injection, therefore, the recombination retes are almost independent of the numbers of QW, as explained earlier. However, the increasing numbers of QW pose additional system resistance, which requires a higher input power. As the consequence, the wall-plug efficiency drops with the increasing numbers of QW. Therefore, the optimal efficiency of 12.8% under 100A/m carrier injection can be accomplished for green emitter with a wavelength of 520 nm using a single QW with a thickness of 3 nm. On the other hand, the carrier injection is about three times larger than 100 A/m under 5V operation. 3-nm single QW device can no longer capture most of the injecting carriers, multiple QWs, in this case, can improve the capture rate and boost the radiative recombination without suffering from quantum-confined Stark effect. Although the system resistance may increase like it was discussed earlier, the increase of carrier concentration dominates the wall-plug efficiency. Therefore, Fig. 12(a) and (b) behaves oppositely in terms of the numbers of QW when the thickness of QW is thicker than 3 nm. The optimal efficiency of 7.4% under 5V operation can be accomplished for green emitter with a wavelength of 520 nm using 5 QWs with a thickness of 3 nm. Notably, 7.4% is the local maximum efficiency that can be achieved. A higher efficiency may be achievable by stacking more QWs (>5) to further improve the capture rate until all of the carriers are fully captured. Yet, the optimal efficiency will be smaller than 12.8% because 5V operation has a higher carrier injection than 100 A/m, which implies a lower IQE due to the efficiency droop and the stronger Auger losses.

Overall, the optimal efficiency of green emitter (520 nm wavelength) that can be achieved under 100 A/m carrier injection is 12.8% using a single QW with a thickness of 3 nm. If the device is designed to operated under a constant bias of 5V, the highest efficiency is 7.4% using 5 QWs with a thickness of 3 nm, but it is a local maximum. A higher number of QW is needed to be investigated. From the analysis, the limiting factors are the polarization (or quantum-confined Stark effect), which limits the radiative recombination rate, and Auger recombination.

- **OPTIMIZATION OF ZINCBLENDE GAN-BASED GREEN LEDS**

Zincblende GaN and its ternary featuring polarization-free nature and expected small Auger coefficient are promising to further boost the optimal efficiency obtained in wurtzite GaN-based green LEDs. Because some of the fundamental properties of zincblende GaN are still unknown, several assumptions were made to continue the zincblende GaN-based green LED simulations.

1. The electron and hole mobilities are identical to wurtzite GaN.
2. The bandgap of zincblende InGaN is obtained using first-principles calculations.
3. Varshini coefficients, α and β, are 0.593 meVK^{-1} and 600K reported from experiment[11].
4. Auger coefficient is assumed to be identical to wurtzite GaN.

5. Band offset ratio of 0.67 extracted from wurtzite InGaN is assumed for zincblende InGaN

The Auger coefficient of wurtzite GaN is employed because there is still no report on the Auger coefficient of zincblende GaN. However, it is important to know the sensitivity of Auger coefficient on the IQE and compare with that of wurtzite GaN-based green LEDs. Fig. 13 shows the IQE of single QW (with 2.5 nm thickness) green LED as a function of carrier injection for zincblende (cubic) GaN and wurtzite (hexagonal) GaN with the Auger coefficients of $2.96 \cdot 10^{-30}$ cm^6s^{-1} (×1) and $2.96 \cdot 10^{-31}$ cm^6s^{-1} (×0.1). It shows that even if the Auger coefficients are the same, the IQE of zincblende GaN is 15% higher than that of wurtzite GaN (see black lines), which can be ascribed to the free of polarization and the smaller bandgap. Even though the Auger coefficients are artificially reduced by an order for both zincblende and wurtzite GaN (see red lines), the IQE of zincblende GaN still outshines that of wurtzite GaN by more than 20% in the carrier injection of 200 A/m. The difference can be further increased with a higher carrier injection.

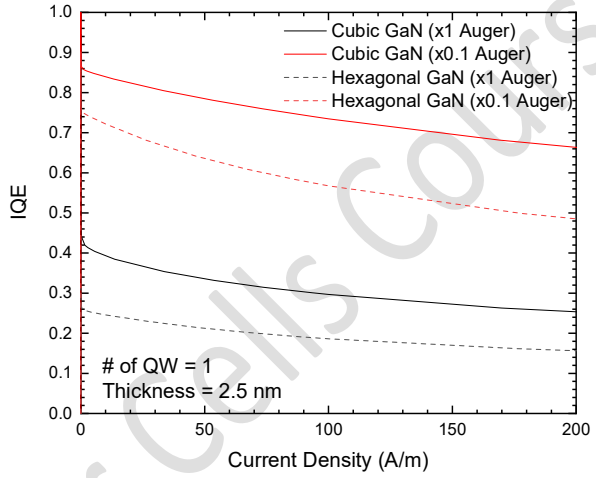

Fig. 13 IQE of single QW (with 2.5 nm thickness) green LED as a function of carrier injection for zincblende (cubic) GaN and wurtzite (hexagonal) GaN with the Auger coefficients of $2.96 \cdot 10^{-30}$ cm^6s^{-1} (×1) and $2.96 \cdot 10^{-31}$ cm^6s^{-1} (×0.1).

Similar to Fig. 12, the zincblende GaN-based green LEDs are optimized by introducing more QWs with different QW thicknesses. Specifically, the numbers of QW from 1 to 5 are focused; while, the QW thickness ranges from 1 nm to 11 nm, which is wider than that of wurtzite counterparts due to the lack of polarization. Fig. 14(a) and (b) demonstrates the wall-plug efficiency of zincblende GaN-based LEDs as a function of the numbers and thickness of QW under a constant carrier injection of 100 A/m and a constant bias of 5V, respectively. White dash lines indicate the peak emission wavelength. Similar to the wurtzite GaN-based LEDs, the QW thickness of zincblende GaN-based LEDs should be thicker than 3 nm for green emitter applications. However, different from Fig. 12, both operation modes show that a higher efficiency is achievable using more QWs with a thicker thickness. Specifically, thick QWs are able to capture more carriers for radiative recombination without suffering from electron-hole spatial separation constrained by quantum-confined Stark effect. Additionally, the Auger recombination rate drops with respect to

the increasing numbers and thickness of QW, which behaves oppositely with that of wurtzite cases. In theory, more carriers imply a stronger Auger recombination rate. However, because zincblende materials have no polarization field, therefore the carriers in the QW have a gaussian distribution instead of a delta-like distribution, where Auger recombination rate is, indeed, dominated by the peak of electron and hole concentrations due to its cubic dependence on carrier concentrations. As the consequence, the Auger recombination rate reduces for thick QWs. Overall, the highest efficiencies of 47.8% and 21.4% can be achieved under the constant carrier injection of 100 A/m and the constant bias of 5V, respectively, which are 3 times more efficient than 12.8% and 7.4% procured using wurtzite GaN-based green LEDs. Notably, the results represent the lower bound that can be achieved because the expected Auger coefficient is smaller than the value used in the simulation. According to the results, thicker QWs (>11 nm) are expected to further increase the wall-plug efficiency.

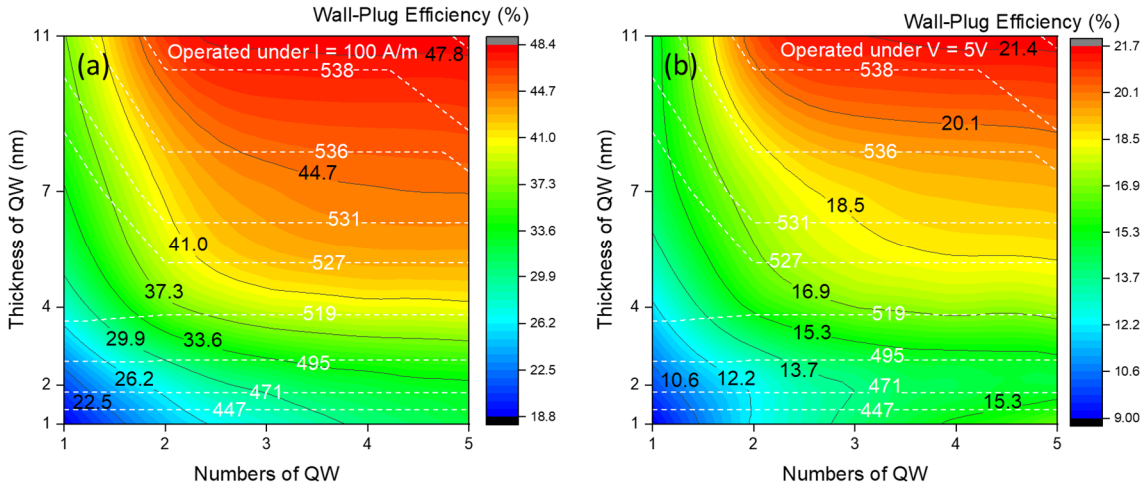

Fig. 14 Wall-plug efficiency of zincblende GaN-based LEDs as a function of the numbers and thickness of QW under (a) a constant carrier injection of 100 A/m and (b) a constant bias of 5V, respectively. White dash lines indicate the peak emission wavelength.

IV. CONCLUSION

In summary, the impact of SRH, radiative, and Auger recombination, electron leakage, polarization, and thermal effect on green gap have been investigated. Auger recombination and polarization are found to be the major culprits. Optimizations in device geometry and materials are needed to bridge the green gap. Wurtzite GaN-based green LEDs are optimized by varying the numbers and thickness of QW. The optimal efficiencies of 12.8% and 7.4% are procured under a constant carrier injection of 100A/m and a constant bias of 5V. To further boost the efficiency with zero polarization, zincblende GaN-based green LEDs are developed and optimized. The optimal efficiencies of 47.8% and 21.4% under a constant carrier injection of 100A/m and a constant bias of 5V show a significant improvement by a factor of 3. Most importantly, the optimal efficiencies are the lower bounds due to the overestimated Auger coefficient used in the simulation. A higher efficiency is feasible by increasing the thickness of QW.

REFERENCES

[1] N. Holonyak and S. F. Bevacqua, *Appl. Phys. Lett.* **1**, 82 (1962).

[2] S. Nakamura, T. Mukai, and M. Senoh, *Appl. Phys. Lett.* **64**, 1687 (1994).

[3] H. Amano, I. Akasaki, T. Kozawa, K. Hiramatsu, N. Sawaki, K. Ikeda, and Y. Ishii, *J. Lumin.* **40**–**41**, 121 (1988).

[4] F. Bernardini, in *Nitride Semicond. Devices Princ. Simul.* (Wiley-VCH Verlag GmbH & Co. KGaA, Weinheim, Germany, n.d.), pp. 49–68.

[5] M. Auf der Maur, A. Pecchia, G. Penazzi, W. Rodrigues, and A. DiCarlo, *Phys. Rev. Lett.* **116**, 027401 (2016).

[6] *Assessment of Solid-State Lighting, Phase Two* (National Academies Press, Washington, D.C., 2017).

[7] Y. C. Shen, G. O. Mueller, S. Watanabe, N. F. Gardner, A. Munkholm, and M. R. Krames, *Appl. Phys. Lett.* **91**, 141101 (2007).

[8] K. T. Delaney, P. Rinke, and C. G. Van De Walle, *Appl. Phys. Lett.* **94**, 5 (2009).

[9] M. Zhang, P. Bhattacharya, J. Singh, and J. Hinckley, *Appl. Phys. Lett.* **95**, 201108 (2009).

[10] L. Wang, X. Meng, J.-H. Song, T.-S. Kim, S.-Y. Lim, Z.-B. Hao, Y. Luo, C.-Z. Sun, Y.-J. Han, B. Xiong, J. Wang, and H.-T. Li, *Chinese Phys. Lett.* **34**, 017301 (2017).

[11] I. Vurgaftman and J. R. Meyer, *J. Appl. Phys.* **94**, 3675 (2003).